

Hot Cutting of Press-Hardened Parts in Different Heat Treatment Regimes



R. Schmidt, A. Rautenstrauch, and V. Kräusel

Abstract Parts made of press-hardened steel are cut in general by laser cutting. Shear cutting at room temperature of materials with a tensile strength above 1,500 MPa is not an alternative due to insufficient tool life quantity. The presented investigation relates to the hot cutting of press-hardenable materials such as 22MnB5 and 34MnB5 and includes the determination of the cutting parameters (measuring rate of 100,000 Hz), the temperature, the formation of the microstructure, and the dimensional accuracy of the cut parts during different heat treatments. The results of this investigation show that, when comparing two process routes, the maximum cutting force was reduced to approximately 70 % when cutting in the austenitic range, the acceleration during the cutting impact was close to zero and the deviations from the target geometry were very small. With regard to the measurement results, hot cutting can be an alternative to laser cutting.

Keywords Hot cutting · Press-hardened steels · Thermal treatment

1 Introduction

In recent years, the use of high-strength press-hardened steel has increased, especially for structural parts of the car body. This is due to the increasing need for weight savings while maintaining the same safety requirements in the automobile. The use of press-hardenable boron–manganese steels offers a promising approach to further optimize the lightweight design of structural components. If a critical cooling rate is taken into account during the hot forming of these steels and the targeted quenching in the cooled forming tool, a martensitic structure with strengths >1,200 MPa is obtained [1].

Due to the high tensile strength, press-hardened parts are difficult to cut with mechanical cutting tools due to high abrasive tool wear and even complete tool breakage. Mechanical cutting represents a conventional shear cutting operation. The

R. Schmidt (✉) · A. Rautenstrauch · V. Kräusel
TU Chemnitz, Chemnitz, Germany
e-mail: rainer.schmidt@mb.tu-chemnitz.de

greatest challenge in the processing of press-hardened sheet metal parts is the very high cutting force and the resulting cutting impact. This results in a high alternating load on the cutting tools, which is manifested as heavy wear on the active cutting elements. As a result, the cutting tools require frequent maintenance, which is associated with high operating and maintenance costs. Laser cutting is currently the most widely used method for cutting press-hardened steel parts. However, laser cutting as a flexible thermal cutting process is very cost-intensive as well as time and energy-consuming [2–4].

The following optimization potentials for the processing of press-hardened steels can be derived from these facts: One approach that is examined in this article is the substitution of the complex laser cutting after press hardening by hot cutting the component in the austenitic state. Currently, only limited experience is available regarding the hot cutting of sheet metal parts made of boron–manganese steels and the corresponding process parameters. Hot cutting offers the possibility to reduce time and operating costs by simultaneously cutting and quenching during forming after previous heating above the austenitizing temperature. Direct quenching in the tool leads to an increase in the tensile strength of the heat-treated and sheared sheet metal part. At the same time, however, the ductility also decreases [5, 6].

In this paper, the influence of the thermal treatment and carbon content of the press-hardenable material on cutting force, cutting impact, part quality, and mechanical properties of hot cut boron–manganese steels is examined. The approach of this work is to punch the sheet metal part in a ductile state to avoid the high dynamic stress on the cutting punch and thus achieve a longer tool life quantity. Of course, the tool heats up with the number of cuts with a consequent change in its strength properties, but this will be initially neglected in this study.

2 Experimental Details

2.1 Selection of Alloys

In this work, a selected group of steel alloys were investigated based on their similarities, e.g. their similar chemical compositions, which are summarized in Table 1. Strip samples with dimensions of $400 \times 30 \times 1.5$ mm were used for all experiments. The manganese–boron steel alloys 22MnB5 and 34MnB5 in supply condition, i.e. cold-rolled, show a ferritic–pearlitic microstructure with the presence of some carbides.

Table 1 Nominal composition of the studied alloys (wt%)

Steel alloy	C	Si	Mn	P	S	Cr	Mo	B	Ti
22MnB5	0.17	0.22	1.19	0.01	0.008	0.12	0.01	0.001	0.03
34MnB5	0.35	0.29	1.28	0.01	0.01	0.17	0.01	0.004	0.03

The 22MnB5 has a carbon content of about 0.17 % and the material 34MnB5 of about 0.35 % (Table 1).

2.2 Punching Tool and Measurement Concept

The tool has two tool halves, which are guided with four columns and dimensioned primary for cutting of ultra-high-strength steels. The tool material Böhler K890 was used for the punch and the selected material for the die was a Böhler S600. The tool has an integrated cutting shock absorption, which was in tests always enabled. The stripes were 5 mm above the cutting die and the distance to the next support surface was 60 mm. Therefore, the cooling of the strips on contact with the tool is negligible. The manual transport of the stripes from the oven to the cutting process needs around about 2 seconds. The diameter of the punch is 10 mm and the constant cutting clearance is 0.2 mm. A constant blank holder force of 90 kN was set and the punch velocity was adjusted with an industry-relevant value of 50 mm/s. The tool was moved path-controlled by a servo-driven spindle press of the company DUNKES [7] (Fig. 1).

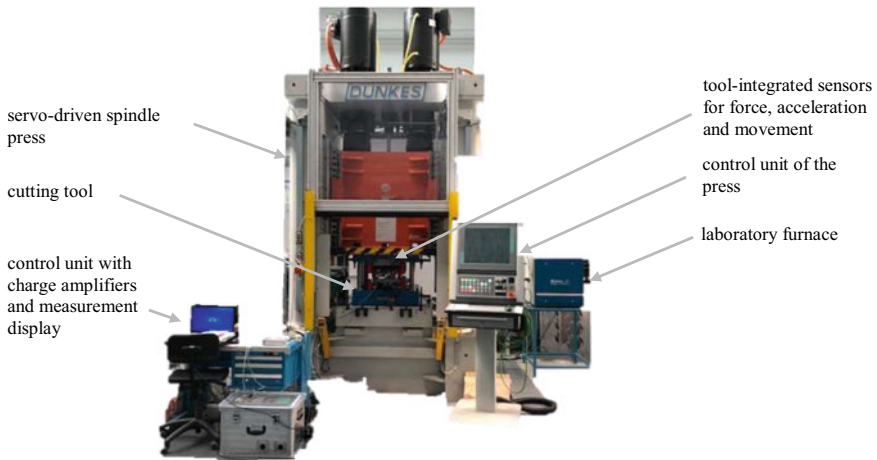


Fig. 1 Experimental setup with the position of measurement sensors. (Color figure online)

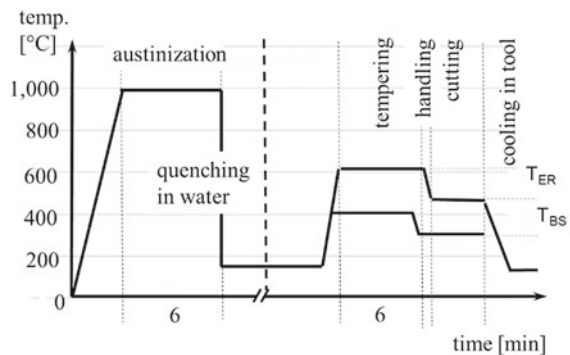
Tool-integrated sensors measure the cutting force, acceleration, and movement. The force sensor is positioned directly above the punch in a special construction to measure the pure cutting force without force shunt and other influencing factors. The position of the sensors for acceleration and movement is near the cutting zone. The controlling and saving of the measurement values implement with a control unit of National Instrument. The selected measurement frequency of 100,000 Hz is necessary to obtain a sufficient resolution of the measurement values, especially in

the area of the cutting impact, and to be able to execute a frequency filtration of the measurement values.

2.3 Thermal Treatments

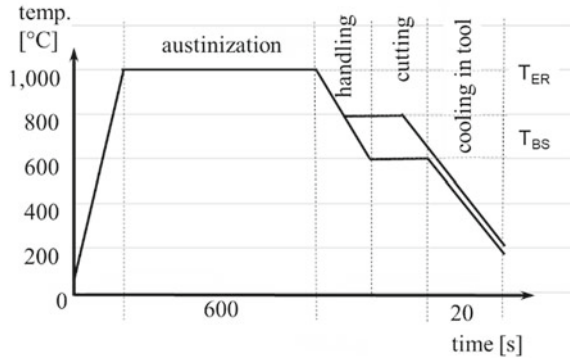
Two different heat treatments were carried out in this work. The first heat treatment route (HTR 1) starts with an austenitization of the test samples at a temperature of 1,000 °C during 10 min and quenched in water by a cooling rate of approximately 10,000 K/s. The hardened strips are then tempered in a furnace in a temperature range between 600 °C and 400 °C for 6 min. The next step is the transfer of the sheet metal strips from the furnace to the cutting tool for punching in the temperature range between 540 °C and 320 °C. After the hot cutting, the tool is opened and the punched sheets are removed for subsequent air cooling to room temperature (Fig. 2).

Fig. 2 Heat treatment route
1—HTR 1



In the second heat treatment route HTR 2, the samples are heated at a temperature of 1,000 °C for 10 min. Afterward, the austenitized samples are transferred from the furnace to the cutting tool and cut between 800 °C and 600 °C. During handling, the samples cool down from the furnace temperature to the cutting temperature at a cooling rate of approximately 14 K/s (Fig. 3).

Fig. 3 Heat treatment route 2—HTR 2

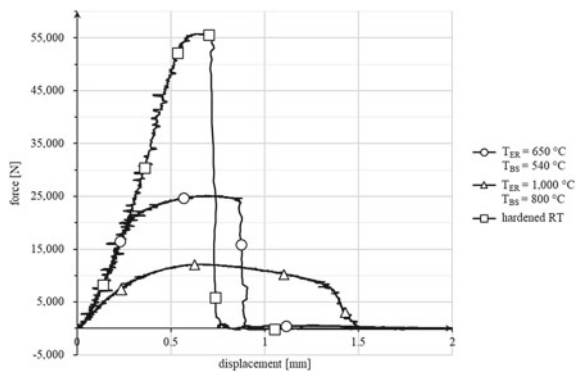


3 Results

3.1 Determination of Cutting Performance

The measurement values were evaluated with a self-developed algorithm in the software MATLAB R2019b and filtered against the noisy frequency with a standard MATLAB filter function. To prepare a comparison of different force–displacement curves, the beginning of the curves with the first increase in cutting force is determined for further investigation. In Fig. 4, three typical force–displacement curves

Fig. 4 Typical force–displacement curves for punching of strips made of 34MnB5



are shown as an example of the tested material 34MnB5 with three different heat treatment routes.

The highest cutting force and the shortest flush-cut amount can be determined when cutting from the hardened strip. The abrupt dropdown of the force by approximately 0.7 mm punch penetration results in the highest measured cutting impact in this study. In comparison, a much more pronounced shear zone can be seen on the hot cut sample due to the better forming capacity and thus material flow. Especially, the

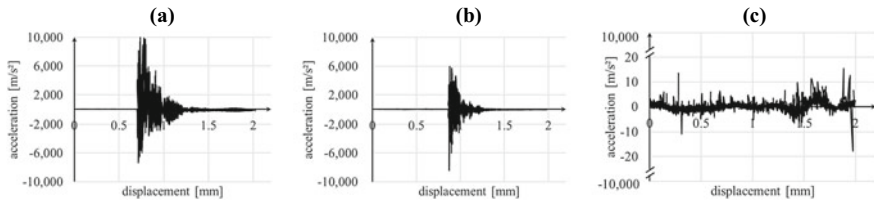
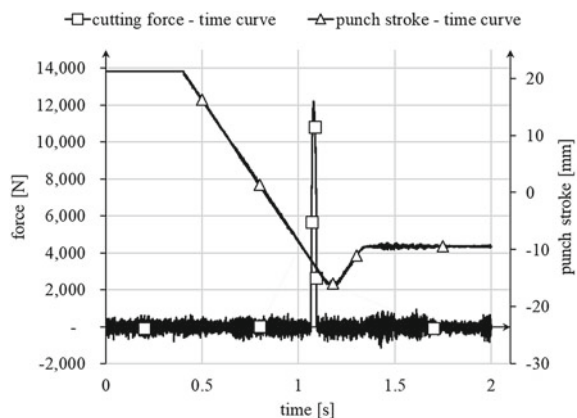


Fig. 5 Acceleration–displacement curves for punching of strips made of 34MnB5 of (a) hardened RT; (b) $T_{ER} = 650\text{ }^{\circ}\text{C}$; $T_{BS} = 540\text{ }^{\circ}\text{C}$; (c) $T_{ER} = 1,000\text{ }^{\circ}\text{C}$; $T_{BS} = 800\text{ }^{\circ}\text{C}$

material 34MnB5 shows an elastic behavior at $800\text{ }^{\circ}\text{C}$ up to a displacement of 0.2 mm. Afterward, the plastic deformation proceeds until the end of the cutting process with a smooth run-out of the force–displacement curve without any recognizable cutting influence (Fig. 5).

As shown in Fig. 6, after punching a hole with a diameter of 10 mm, the punch enters the die 1 mm and remains at the bottom dead center for one second. Then the punch moves out of the die and the sheet strip while the blank holder continues to press the workpiece onto the die. At this point, the material cools to martensite start temperature and hardening occurs. This is followed by the opening of the tool and the sheet strip is removed. For both the HTR 2 and the uncured material, an increase in retraction force was noticeable after cutting. This suggests that at the time of cutting, no hardening of the material took place during the process route HTR 2 because the martensite start temperature has not yet been reached.

Fig. 6 Development of cutting force for cutting of 34MnB5 at HTR 2



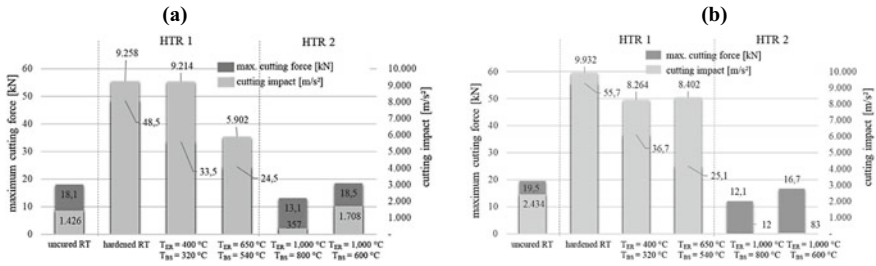


Fig. 7 Maximum cutting force and cutting impact of a) 22MnB5; b) 34MnB5

3.2 Determination of the Maximum Cutting Force and Cutting Impact

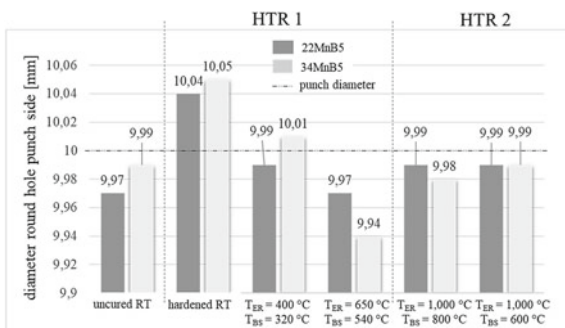
To determine the maximum cutting force and the cutting impact, the interference signals are filtered with the MATLAB filter function. The cutting impact values after the break are included in the evaluation. The results in Fig. 7 show that the highest maximum cutting forces correlate with the highest measured cutting impact values. Furthermore, it is found that the lowest cutting forces show a correlation with the lowest measured cutting impact values. The results were found to be independent of the material. When cutting hardened steels according to heat treatment route 1, higher cutting forces and higher cutting impact values are recorded compared with heat treatment route 2. In contrast, the lowest maximum force of 12.1 kN was obtained during hot cutting of the material 34MnB5 along HTR 2 at a cutting temperature of 800 °C. The cutting impact could not be measured for this low cutting force.

3.3 Determination of Cutting Quality

In addition to the investigation of Neumayer et al. [6] and So et al. [8], the diameters of the round holes are measured optically with a Keyence microscope VHX-600 with a deviation of about 0.02 mm. The following Fig. 8 shows the diameter of the hole from the punch side compared to the punch diameter.

For both investigated materials, a similar diameter of the perforated stripe on the side of the punch could be measured for the respective heat treatment routes. The hole in the hardened stripe increased significantly after cutting, which is why no retraction forces were measured. In contrast, the hole in the hardened stripe, which was reheated to 650 °C and cut at 340 °C, was reduced to 9.94 and 9.97 mm respectively. As a result of HTR 1, a retraction force of approximately 500 N could be measured during cutting for both materials examined. In particular, the diameters determined according to HTR 2 scarcely changed compared to the punch diameter, taking into account the measurement inaccuracy. Since no retraction forces greater

Fig. 8 Round hole diameter versus punch diameter



than 100 N were measured, no abrasive wear at higher stroke rates is likely to be detected.

3.4 Determination of the Mechanical Properties

To investigate the influence of the heat treatment routes on the mechanical properties, the cut specimens were embedded, subjected to a hardness test and metallographic examination. Vickers Hardness tests were performed using the load range HV 1. The experimentally determined Vickers hardness of the heat-treated sheets is shown in Fig. 9. The samples were prepared for micrographs. Microstructural analysis was performed using optical microscopy from ZEISS.

Samples were chemically etched using 3 % Nital solution. In heat treatment route 1 after austenitization followed by quenching in water, both materials show a clear hardening, for the 22MnB5 of 640 HV1 and for the 34MnB5 of 738 HV1. The microstructure of both hardened materials shows martensite (Figs. 10 and 11). Because of reheating to 650 and 400 °C, the material relaxes and after cooling, it has a reduced hardness. The material 22MnB5 shows 365 HV1 at 650 °C and 484 HV1 at 400 °C. In addition, a hardness of 332 HV1 for the material 34MnB5 after heat treatment at 650 °C and 528 HV1 after 400 °C (Fig. 9) was measured. The

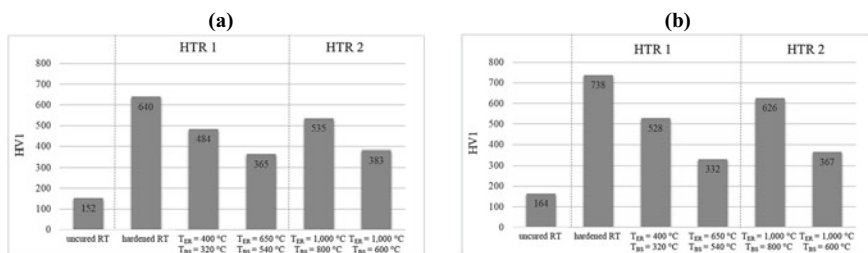


Fig. 9 Hardness values HV1 for **a** 22MnB5; **b** 34MnB5

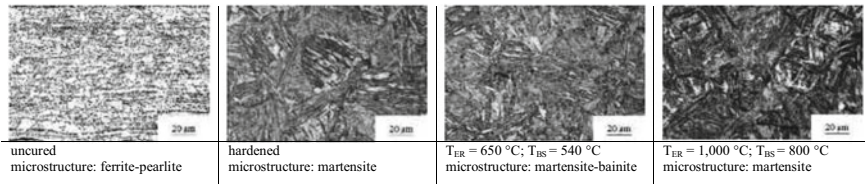


Fig. 10 Microstructure development for 22MnB5

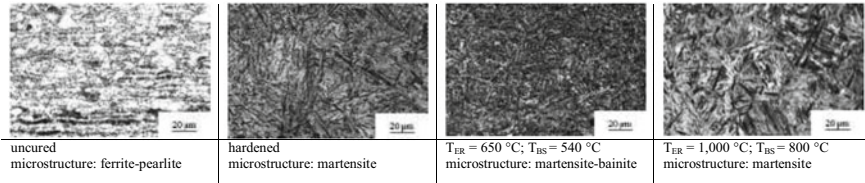


Fig. 11 Microstructure development for 34MnB5

microstructure showed a martensitic–bainitic structure in both materials due to the subsequent tempering (Figs. 10 and 11).

Along heat treatment route 2, the materials 22MnB5 and 34MnB5 are heated to 1,000 °C in the furnace, hot cutting in the tool, and cooled to room temperature. After heat treatment and cutting, the material 22MnB5 has a hardness of 535 HV1 at 800 °C and 383 HV1 at a cutting temperature of 600 °C. Because of the heat treatment, the material has a martensitic structure after treatment. The material 34MnB5 shows, after austenitization and hot cutting a hardness of 626 HV1 at 800 °C and a hardness of 367 HV1 at a cutting temperature of 600 °C. The microstructure shows also here a martensitic structure due to the heat treatment (Figs. 9, 10, and 11).

4 Conclusions and Outlook

The presented results show that the maximum cutting force as well as the cutting impact are considerably reduced due to the hot cutting of boron–manganese steels. Along heat treatment route 1, an improvement in mechanical cutting for press-hardened materials could be achieved. For example, for the press-hardened 22MnB5, a reduction of the cutting force by up to 50 % was achieved by cutting at a cutting temperature of 650 °C.

The measured cutting impact close to zero has no influence on the tool life quantity. With regard to tool production, it can be deduced for hot cutting to use a tool material with higher heat resistance. Small deviations in the cutting clearance are negligible in route 2 and allow a greater margin with regard to the tool tolerances.

With the heat treatment route 2, proof could be provided that in a direct heat treatment process, the process heat can be used for hot cutting and a martensitic microstructure can be set. For this purpose, approaches are being pursued to combine the hot cutting with the press-hardening process in one step and to integrate the hot cutting in a press-hardening tool.

Acknowledgments The authors acknowledge Salzgitter Flachstahl GmbH, especially Dr. Stefan Mütze, for providing the 34MnB5 material and acknowledge AWEBA Werkzeugbau GmbH Aue, especially Dipl.-Ing Thomas Aurich, for providing the cutting tool.

References

1. Neugebauer R, Schieck F, Rautenstrauch A and Bach M (2011) Hot sheet metal forming: the formulation of graded component characteristics based on strategic temperature management for tool-based and incremental forming operations. *CIRP J Man Sci Technol* 4:180–188
2. Krönauer B, Hirsch M, Golle R, Hoffmann H, Golle M and Jesner G (2010) Beschneiden von pressgehärteten Blechen: Ultrahochfestes 22MnB5-Blech im Scherschneidprozess. *ZWF Zeitschrift für wirtschaftlichen Fachbetrieb*, 26–31
3. Mori K, Maeno T, and Fuzisaka S (2012) Punching of ultra-high strength steel sheets using local resistance heating of shearing zone. *J Mater Process Technol* 212:534–540
4. Mori K, Saito S and Maki S (2008) Warm and hot punching of ultra high strength steel sheet. *CIRP Ann - Manuf Technol* 57:321–324
5. Hoffmann H, So H and Steinbeiss H (2007) Design of hot stamping tools with cooling system. *CIRP Ann* 56:269–72
6. Neumayer FF, Vogt S, Gueffroy M, Jesner G, Kelsch R, Sommer A, Golle R, Volk W (2019) *Proc Man* 29:345–352
7. Nestler M, Galiev E, Schmidt R, Psyk V, Winter S and Kräusel V (2020) Scherschneiden höchstfester Stähle mit fluidischem Gegenhalter. *ZWF Zeitschrift für wirtschaftlichen Fachbetrieb Jahrg* 115:7–8
8. So H, Faßmann D, Hoffmann H, Golle R and Schaper M (2012) An investigation of the blanking process of the quenchable boron alloyed steel 22MnB5 before and after hot stamping process. *J Mat Process Technol* 212:437–449